Computer Assisted Mechanics and Engineering Sciences, 4: 257–281, 1997.

Optimal remodelling of truss structures (simulation by virtual distortions)

Przemysław Kołakowski and Jan Holnicki-Szulc
Institute of Fundamental Technological Research,
Świętokrzyska 21, 00-049 Warsaw, Poland

(Received February 25, 1997)

Optimal remodelling for least-weight trusses under single as well as multi-load state and limits imposed on local strains is considered. The so called Virtual Distortion Method is applied to simulate process of structural remodelling through fictitious "virtual distortions". In effect, applying knowledge of strains induced by virtual distortions modelling material redistribution, analytical formulas for sensitivity analysis and remodelling simulation process can be obtained. Various algorithms for the VDM-based structural remodelling have been proposed and tested on examples of elastic and elasto-plastic trusses.

1. INTRODUCTION

The problem of optimal design of a truss structure for minimum compliance leads to determination of cross-sectional areas for members of loaded, so called *ground structure* with defined initial topology. The same problem can be formulated equivalently as minimization of the total material volume subject to limits imposed on local strains. The problem was formulated first by Michell (Ref. [1]) and then discussed by many researchers on the basis of various approaches during last decades. A comprehensive review of the published results can be found in papers by Topping (Ref. [5]) and Bendsoe et al. (Ref. [2]). The analytical approach (e.g. Lewinski et al., Ref. [4]) on one hand and the powerful numerical tool, based on the so-called homogenization method applied first by Bendsoe and Kikuchi (Ref. [3]) on the other, are examples of methods (still under development) for optimal layout design. In fact, the well known ground structure method with defined initial configuration of the structure leads to optimal design of structural topology through the simple so called sizing problem, modifying cross-sectional areas (including the possibility of zero bar areas).

The goal of this paper is verification of numerical efficiency of the approach based on the so called *Virtual Distortion Method* (Ref. [6]) to optimal structural remodelling. The VDM takes advantage of a fictitious field of *virtual distortions* (deformation-like loading with the influence on the structure analogous to a thermal field) in the simulation of material redistribution. Stresses induced by virtual distortions are self-equilibrated while strains are compatible. As it is possible to determine direct relation between material redistribution and the corresponding virtual distortions (causing the same modifications of strains and stresses), the whole remodelling process can be simulated through these fictitious distortions with analytical formulas making gradient calculation available. The main concept, already postulated (Refs. [6, 7]) is verified in this paper with use of various algorithms and analytical formulas for sensitivity analysis. Applications to multi-load as well as elasto-plastic cases are also searched. This last case has special potential applications, as the "side effect" for optimal remodelling of elasto-plastic structures is significant expansion of the plastic zone (rather than gain due to material volume saving), which can be desired in design for maximum load capacity. In the case of extreme loading the energy absorption of the properly remodelled structure can be much higher. Combining this result with the concept of *structural fuses* (devices allowing generation of plastic-like distortions in a controlled way, Ref. [8]) the idea of safe structure, self-adapting to various extreme loadings, can be considered.

2. Virtual distortion method approach in simulation of structural remodelling

Let us focus on presenting the basic concept of the Virtual Distortion Method (cf. Ref. [8]) in simulation of structural remodelling. A simple three-bar truss has been chosen for demonstration of the main idea. The vertical element of the *initial structure* shown in Fig. 1, has been subjected to an initial elongation. Let us call the corresponding deformation of the vertical element (in isolation), expressed by ε^0, a *virtual distortion*. This initially deformed member built into the structure provokes a *self-equilibrated* state of stresses with residual deformation ε^R (see the *prestressed structure* in Fig. 1). The virtual distortion can be decomposed into two parts: $\varepsilon^0 = \varepsilon^{0c} + \varepsilon^{0r}$. The component ε^{0c} is responsible for the compatible deformation of the structure while the component ε^{0r} causes the self-equilibrated stress state in the structure.

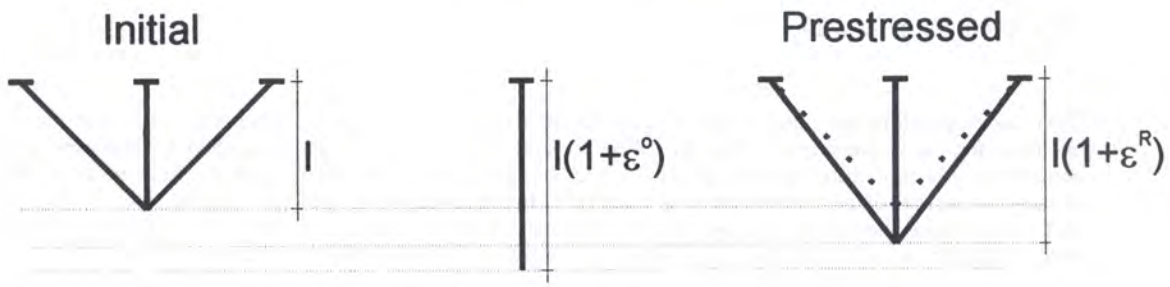

Fig. 1. Structure with imposed virtual distortions

Then, let us apply external force-type load P to the structure shown in Fig. 2. It generates the deformation denoted by ε^L in the *loaded* structure. Superposing the two states of the *prestressed* and the *loaded* structure we get, as a result, a distorted structure.

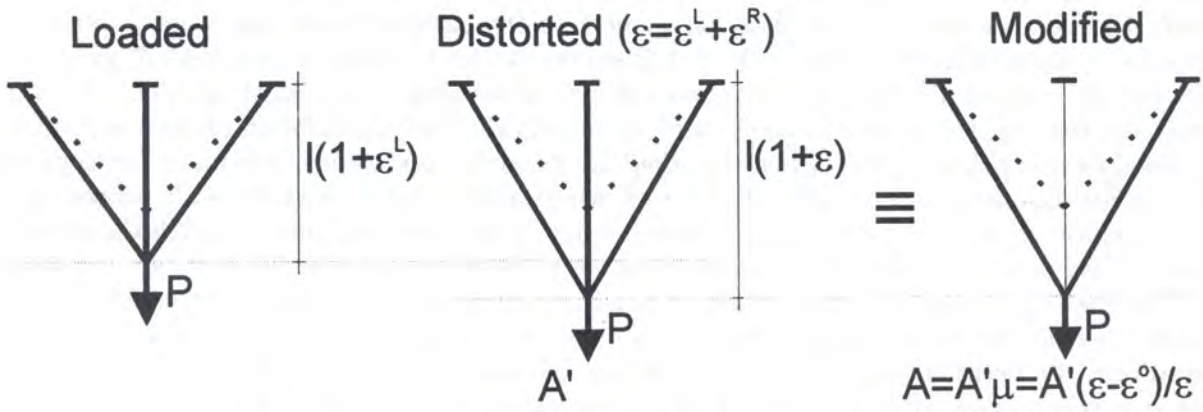

Fig. 2. Equivalence between "distorted" and "modified" structure

It is postulated now that (as shown in Fig. 2) the *distorted structure* is identical in terms of final deformations ε and internal forces with a *modified structure* (with the cross-sectional area in the vertical element changed from A' to A).

In any truss structure subjected to external load and virtual distortion ε^0 state, strains and stresses, calculated with respect to the initial cross-sections A_i', can be expressed as follows:

$$\begin{aligned} \sigma_i &= E_i(\varepsilon_i - \varepsilon_i^0) = E_i\left(\varepsilon_i^L + \sum_j (D_{ij} - \delta_{ij})\varepsilon_j^0\right), \\ \varepsilon_i &= \varepsilon_i^L + \sum_j D_{ij}\varepsilon_j^0, \end{aligned} \tag{1}$$

where D_{ij} (influence matrix) denote deformations caused in the members i by the unit virtual distortions $\varepsilon_j^0 = 1$ generated in members j and ε_i^L denotes deformations due to the external load.

The above requirement that both internal forces as well as deformations calculated for two structural models: the *modified structure* (with modified design variables), and the *distorted structure* (with imposed virtual distortions) are equal, leads to the following formulas:

$$\begin{aligned} P_i &= E_i A_i'(\varepsilon_i - \varepsilon_i^0)\,, \\ P_i &= E_i A_i \varepsilon_i\,, \end{aligned} \tag{2}$$

where $()'$ means initial, unmodified design variable. Comparing right hand-sides of Eqs. (2), the following expression for modelling of cross-sectional modification through virtual distortions can be derived:

$$\mu_i \equiv \frac{A_i}{A_i'} = \frac{\varepsilon_i - \varepsilon_i^0}{\varepsilon_i}\,. \tag{3}$$

Analogously (by applying modifications of E_i instead of A_i in Eqs. (2)), we can get expression for simulation of Young's modulus modification:

$$\eta_i \equiv \frac{E_i}{E_i'} = \frac{\varepsilon_i - \varepsilon_i^0}{\varepsilon_i}\,. \tag{4}$$

Also, substituting $\varepsilon_i = \Delta l/l = \Delta l'/l'$, we can get expression for simulation of member length modification:

$$\lambda_i \equiv \frac{l_i'}{l_i} = \frac{\varepsilon_i - \varepsilon_i^0}{\varepsilon_i}\,. \tag{5}$$

Natural constraints imposed on the above ratios:

$$\mu_i \geq 0\,, \quad \eta_i \geq 0\,, \quad \lambda_i \geq 0\,, \tag{6}$$

lead to the following condition (for non-prestressed structure): $\varepsilon_i^0 = 0$ if $\varepsilon_i = 0$, which can also be expressed as the requirement: $\sigma_i \varepsilon_i \geq 0$.

In conclusion, for any modification of material distribution a virtual distortion state simulating this redesign can be found. To this end, Eq. $(1)_2$ has to be substituted into (3) and solved with respect to ε_i^0.

3. Problem formulation

The problem of optimal remodelling of a truss structure can be formulated as follows:

$$\min V = \min \sum_i A_i l_i \tag{7}$$

subject to the following constraints:

$$A_i \geq 0 \quad \text{and} \quad |\varepsilon_i| \leq \varepsilon^u\,, \tag{8}$$

where ε^u denotes arbitrary limit imposed on strains. These strains are related through the geometrical relations to nodal displacements u_j:

$$\varepsilon_i = G_{ij} u_j \tag{9}$$

satisfying the equilibrium conditions:

$$K_{ij} u_j = p_i\,, \tag{10}$$

where p_i denotes external load and G_{ij}, K_{ij} are the geometric matrix and the global stiffness matrix, respectively.

Taking advantage of the VDM approach the above problem (7)–(10) can be converted into the following:

$$\min V = \min \sum_i \mu_i A_i' l_i = \min \sum_i \frac{\varepsilon_i - \varepsilon_i^0}{\varepsilon_i} A_i' l_i \tag{11}$$

subject to the constraints:

$$\mu_i = \frac{\varepsilon_i - \varepsilon_i^0}{\varepsilon_i} \geq 0\,, \tag{12}$$

$$|\varepsilon_i| \leq \varepsilon^u\,, \tag{13}$$

where the last one can be expressed alternatively as follows:

$$h_i = 1 - \left(\frac{\varepsilon_i}{\varepsilon^u}\right)^2 \geq 0\,. \tag{14}$$

The global stresses and strains in distorted structure are expressed through Eq. (1) and therefore the requirements of compatible deformations (9) and equilibrated stresses (10) are satisfied as superposition of structural response due to external load and self-equilibrated stresses, and compatible strains caused by the virtual distortions. Substituting Eq. $(1)_2$ to (11), (12) and (14) the nonlinear optimization problem (the objective function as well as constraints) with virtual distortions as design variables can be formulated and this formulation will be applied in our approach to the remodelling problem.

Alternatively, substituting Eq. $(1)_2$ into the formula defining material redistribution μ_i (cf. (3)) we get the following set of equations describing relation between material redistribution and virtual distortions:

$$\sum_j \left[(1-\mu_i)D_{ij} - \delta_{ij}\right]\varepsilon_j^0 = -(1-\mu_i)\varepsilon_i^{\mathrm{L}}\,. \tag{15}$$

Now, the optimal remodelling problem can be converted into the formulation with two sets of design variables: μ_i and ε_i^0. The objective function (11) (expressed through μ_i) as well as inequality constraints (12) and (13) (expressed through μ_i and ε_i^0, respectively) are linear and the whole nonlinearity of the problem is cumulated in the additional constraint (15). The solution of this problem is expected on the boundary, with n (the number of structural members) active constraints (12), (13). This, however, is possible for any truss structure if constraints (12) are active for a m element set B_1 of members and constraints (13) are active for the remaining $(n-m)$-element set B_2 of structural members. The formula (15) can be then expressed as follows:

$$\begin{array}{r} m\{ \\ n-m\{ \end{array} \left[\begin{array}{c|c} \mathbf{D}-\mathbf{I} & (\mathbf{I}-\boldsymbol{\mu})\mathbf{D} \\ \hline \mathbf{D} & (\mathbf{I}-\boldsymbol{\mu})\mathbf{D}-\mathbf{I} \end{array}\right] \left[\begin{array}{c} \boldsymbol{\varepsilon}^{01} \\ \hline \boldsymbol{\varepsilon}^{02} \end{array}\right] = \left[\begin{array}{c} -\boldsymbol{\varepsilon}^{\mathrm{L}} \\ \hline -(\mathbf{I}-\boldsymbol{\mu})\boldsymbol{\varepsilon}^{\mathrm{L}} \end{array}\right], \tag{16}$$

where the first m equations impose conditions on ε_i^0 due to requirement $\sigma_i = 0$ for elements from the set B_1, where $\mu_i = 0$, while the $n-m$ last equations allow us to impose relations on ε_i^0 and μ_i due to the condition $\varepsilon_i = \varepsilon_i^{\mathrm{L}} + \sum_j D_{ij}\varepsilon_j^{01} + \sum_j D_{ij}\varepsilon_j^{02} = \varepsilon^u$ for elements from the set B_2 and in view of (3) can be expressed as follows:

$$(1-\mu_i)\varepsilon_i^{(2)} = \varepsilon_i^{02}\,, \quad i = m+1, m+2, \ldots, n\,. \tag{17}$$

Knowing solution μ_i of our optimal remodelling problem with active constraints (12) and (13), the corresponding virtual distortions ε_i^0 are related to μ_i through $n-m$ equations (17) and then, through the m first equations (16) where ε_i^{02} is already known. Note, that the rank of the matrix

$[\mathbf{D}-\mathbf{I}]$ is not bigger than the truss redundancy. The optimal remodelling problem is, in fact, based on determination of such $n-m$ element isostatic substructure (therefore, also determination of sets B_1 and B_2) that the corresponding objective function (11) is minimized.

In case of several load states, where $\varepsilon_i^{\mathrm{L}k}$ describe K $(k=1,2,\ldots,K)$ states of deformations, the uniquely defined, dominant (with maximal strain intensity) load state $\varepsilon_i^{\mathrm{L}k'}$ for each element i can be determined. Also K different final strain states ε_i^k and distortion states $\varepsilon_i^{\mathrm{o}k}$ simulating the same material redistribution μ_i can be introduced and applied in the optimal remodelling algorithm. Determining modifications of distortions (therefore also modifications of μ_i, due to Eq. (3)) on the basis of the dominant states $\varepsilon_i^{k'}$, $\varepsilon_i^{\mathrm{o}k'}$ (corresponding to the dominant load for the element i) the missing components $\varepsilon_i^{\mathrm{o}k}$ can be calculated from the following equations:

$$\mu_i = \frac{\varepsilon_i^k - \varepsilon_i^{\mathrm{o}k}}{\varepsilon_i^k}. \tag{18}$$

4. VDM-BASED SENSITIVITY ANALYSIS

Let us take advantage of the VDM approach to the nonlinear optimal remodelling problem (11), (12), (14). One possibility is a gradient optimization method with sensitivity calculated analytically. Taking into account formulas (1) gradients of stresses and strains with respect to $\varepsilon_j^{\mathrm{o}}$ are the following:

$$\begin{aligned} \frac{\mathrm{d}\sigma_i}{\mathrm{d}\varepsilon_j^{\mathrm{o}}} &= E_i(D_{ij}-\delta_{ij}), \\ \frac{\mathrm{d}\varepsilon_i}{\mathrm{d}\varepsilon_j^{\mathrm{o}}} &= D_{ij}. \end{aligned} \tag{19}$$

Now, gradient of material density μ_i with respect to virtual distortions can be calculated from relation (3):

$$\frac{\mathrm{d}\mu_i}{\mathrm{d}\varepsilon_j^{\mathrm{o}}} = -\frac{\delta_{ij}\varepsilon_i - \varepsilon_i^{\mathrm{o}}\dfrac{\partial\varepsilon_i}{\partial\varepsilon_j^{\mathrm{o}}}}{{\varepsilon_i}^2} \tag{20}$$

or making use of $(19)_2$:

$$\frac{\mathrm{d}\mu_i}{\mathrm{d}\varepsilon_j^{\mathrm{o}}} = \frac{\varepsilon_i^{\mathrm{o}}D_{ij} - \varepsilon_i\delta_{ij}}{{\varepsilon_i}^2}, \tag{21}$$

Finally, all needed gradients of the objective function and the constraints with respect to design variables are the following:

$$\frac{\mathrm{d}V}{\mathrm{d}\varepsilon_j^{\mathrm{o}}} = \sum_i \frac{\partial V}{\partial\mu_i}\frac{\partial\mu_i}{\partial\varepsilon_j^{\mathrm{o}}} = \sum_i A_i' l_i \frac{\varepsilon_i^{\mathrm{o}}D_{ij} - \varepsilon_i\delta_{ij}}{{\varepsilon_i}^2}, \tag{22}$$

$$\frac{\mathrm{d}\mu_i}{\mathrm{d}\varepsilon_j^{\mathrm{o}}} = \frac{\varepsilon_i^{\mathrm{o}}D_{ij} - \varepsilon_i\delta_{ij}}{{\varepsilon_i}^2}, \tag{23}$$

$$\frac{\mathrm{d}h_i}{\mathrm{d}\varepsilon_j^{\mathrm{o}}} = -\frac{2}{(\varepsilon^u)^2}\varepsilon_i D_{ij}. \tag{24}$$

Note, that in the sensitivity analysis, the main numerical cost in gradient optimization methods is relatively cheap in our approach. The influence matrix $\mathbf{D}$ is calculated once, at the very beginning, and then all gradients, dependent on current states of strains and virtual distortions, can be determined from the above formulas during the entire optimization process.

5. REMODELLING OF ELASTO-PLASTIC STRUCTURES

Let us now extend our considerations on the remodelling process for elasto-plastic truss structures. The superposition of plastic-like component β_i^o of virtual distortions, simulating nonlinear member behaviour, with distortions ε_i^o, modelling modifications of design variables, turns out to be productive in this case.

The strains and stresses, calculated with respect to initial cross-sections, can be expressed as follows (cf. Eq. (1)):

$$\begin{aligned} \sigma_i &= E_i(\varepsilon_i - \varepsilon_i^o - \beta_i^o) = E_i\left(\varepsilon_i^L + \sum_j (D_{ij} - \delta_{ij})\varepsilon_j^o + \sum_p (D_{ip} - \delta_{ip})\beta_p^o\right), \\ \varepsilon_i &= \varepsilon_i^L + \sum_j D_{ij}\varepsilon_j^o + \sum_p D_{ip}\beta_p^o, \end{aligned} \tag{25}$$

and the corresponding derivatives take the following form:

$$\begin{aligned} &\frac{\mathrm{d}\sigma_i}{\mathrm{d}\varepsilon_j^o} = E_i(D_{ij} - \delta_{ij}), \qquad &&\frac{\mathrm{d}\sigma_i}{\mathrm{d}\beta_p^o} = E_i(D_{ip} - \delta_{ij}), \\ &\frac{\mathrm{d}\varepsilon_i}{\mathrm{d}\varepsilon_j^o} = D_{ij}, &&\frac{\mathrm{d}\varepsilon_i}{\mathrm{d}\beta_p^o} = D_{ip}. \end{aligned} \tag{26}$$

The subscripts j and p in the above formulas run through all modified and plastified members, respectively. Taking advantage of two expressions for the internal forces applied for *distorted* and *modified* structure (cf. Eqs. (2)) with redesigned cross-sections from A_i' to A_i:

$$\begin{aligned} P_i &= E_i A_i'(\varepsilon_i - \varepsilon_i^o - \beta_i^o), \\ P_i &= E_i A_i(\varepsilon_i - \beta_i^o), \end{aligned} \tag{27}$$

(where components of ε_i^o, β_i^o are non-zero only in distorted or plastified members, respectively), the formula analogous to Eq. (3) can be derived:

$$\mu_i \equiv \frac{A_i}{A_i'} = \frac{\varepsilon_i - \varepsilon_i^o - \beta_i^o}{\varepsilon_i - \beta_i^o}. \tag{28}$$

Analogous formulas for other design variables, e.g. $\eta_i = E_i/E_i'$, $\lambda_i = l_i'/l_i$ can be determined.

$$\begin{aligned} \eta_i &\equiv \frac{E_i}{E_i'} = \frac{\varepsilon_i - \varepsilon_i^o - \beta_i^o}{\varepsilon_i - \beta_i^o}, \\ \lambda_i &\equiv \frac{l_i'}{l_i} = \frac{\varepsilon_i - \varepsilon_i^o - \beta_i^o}{\varepsilon_i - \beta_i^o}. \end{aligned} \tag{29}$$

The relations (28) and (29) have to be completed with the following constraints:

$$\mu_i \geq 0, \quad \eta_i \geq 0, \quad \lambda_i \geq 0, \tag{30}$$

respectively. They lead to the following condition $\varepsilon_i^o = 0$ if $\varepsilon_i - \beta_i^o = 0$. The gradient of μ_i with respect to ε_j^o can be calculated from Eq. (28):

$$\frac{\mathrm{d}\mu_i}{\mathrm{d}\varepsilon_j^o} = -\frac{\delta_{ij}(\varepsilon_i - \beta_i^o) - \varepsilon_i^o \dfrac{\partial(\varepsilon_i - \beta_i^o)}{\partial \varepsilon_j^o}}{(\varepsilon_i - \beta_i^o)^2} \tag{31}$$

and making use of Eq. $(25)_2$:

$$\frac{\mathrm{d}\mu_i}{\mathrm{d}\varepsilon_j^{\mathrm{o}}} = \frac{\varepsilon_i^{\mathrm{o}}\left(D_{ij} - \dfrac{\partial\beta_i^{\mathrm{o}}}{\partial\varepsilon_j^{\mathrm{o}}}\right) - (\varepsilon_i - \beta_i^{\mathrm{o}})\delta_{ij}}{(\varepsilon_i - \beta_i^{\mathrm{o}})^2}. \tag{32}$$

Let us now formulate a remodelling approach for elasto-plastic material behaviour. Such analysis can be performed for multi-load cases only. The reason is that in case of a single load applied to the structure we finally arrive at an isostatic (equally stressed) substructure. This means that we found an optimal structure which cannot be improved any more in terms of weight. Analyzing a multi-load case we are searching such a substructure which consists of members stressed to an imposed limit in at least one of the applied load states. This is so called *fully stressed design*. If the arbitrarily imposed limit matches the yielding limit then we cope with plastic behaviour of the optimal structure. However, there are still elements which work within elastic range in each of the applied load states. The concept of plastic remodelling is to bring to yielding as many of the members of optimal elastic structure as possible in each load state.

Thus the optimal remodelling problem for multi-load, elasto-plastic case can be expressed through virtual distortions in the form:

$$\min V = \min \sum_i \frac{\varepsilon_i^{k'} - \beta_i^{\mathrm{o}} - \varepsilon_i^{\mathrm{o}k'}}{\varepsilon_i^{k'} - \beta_i^{\mathrm{o}}} A_i' l_i \tag{33}$$

subject to the following non-linear constraints:

$$\mu_i = \frac{\varepsilon_i^{k'} - \beta_i^{\mathrm{o}} - \varepsilon_i^{\mathrm{o}k'}}{\varepsilon_i^{k'} - \beta_i^{\mathrm{o}}} \geq 0, \tag{34}$$

$$h_i = 1 - \left(\frac{\sigma_i^k}{\sigma^u}\right)^2 \geq 0, \tag{35}$$

$$b_i = \beta_i^{\mathrm{o}}\sigma_i^{k'} \geq 0, \tag{36}$$

where $\sigma^u = E\varepsilon^u$, ε_i^k and σ_i^k are defined by Eqs. (25) for all load states $k = 1, 2, \ldots, K$. The symbol k' denotes the dominant (with maximal stress intensity), uniquely chosen load state for the element i. Note that constraints $(35)_2$ are imposed on stresses, rather than strains (cf. (14)) and that constraints (36) assure that plastic distortions β_i^{o} are generated due to local energy dissipation. It is assumed that plastic distortion β_i^{o} is generated only for the dominant (for the element i) load state and remains constant for other load states while distortions $\varepsilon_i^{\mathrm{o}k}$ have to be tailored to all load states in order to simulate the same structural remodelling μ_i. However, having determined $\varepsilon_i^{\mathrm{o}k'}$ (for the dominant load state, therefore having also μ_i) the missing components $\varepsilon_i^{\mathrm{o}k}$ can be calculated from the following equations:

$$\mu_i = \frac{\varepsilon_i^k - \beta_i^{\mathrm{o}} - \varepsilon_i^{\mathrm{o}k}}{\varepsilon_i^k - \beta_i^{\mathrm{o}}}. \tag{37}$$

The gradients for the objective function (33) and constraints (34)–(36) with respect to $\varepsilon_j^{\mathrm{o}}$ and β_j^{o} (for any load state k) take the following forms, respectively:

$$\frac{\mathrm{d}V}{\mathrm{d}\varepsilon_j^{\mathrm{o}}} = \sum_i \frac{\varepsilon_i^{\mathrm{o}}\left(D_{ij} - \dfrac{\partial\beta_i^{\mathrm{o}}}{\partial\varepsilon_j^{\mathrm{o}}}\right) - (\varepsilon_i - \beta_i^{\mathrm{o}})\delta_{ij}}{(\varepsilon_i - \beta_i^{\mathrm{o}})^2} A_i' l_i,$$

$$\frac{\mathrm{d}V}{\mathrm{d}\beta_j^{\mathrm{o}}} = \sum_i \frac{\varepsilon_i^{\mathrm{o}}(D_{ij} - \delta_{ij}) - \dfrac{\partial\varepsilon_i^{\mathrm{o}}}{\partial\beta_j^{\mathrm{o}}}(\varepsilon_i - \beta_i^{\mathrm{o}})}{(\varepsilon_i - \beta_i^{\mathrm{o}})^2} A_i' l_i,$$

$$\frac{\mathrm{d}\mu_i}{\mathrm{d}\varepsilon_j^{\mathrm{o}}} = \frac{\varepsilon_i^{\mathrm{o}}\left(D_{ij} - \frac{\partial\beta_i^{\mathrm{o}}}{\partial\varepsilon_j^{\mathrm{o}}}\right) - (\varepsilon_i - \beta_i^{\mathrm{o}})\delta_{ij}}{(\varepsilon_i - \beta_i^{\mathrm{o}})^2}, \qquad \frac{\mathrm{d}\mu_i}{\mathrm{d}\beta_j^{\mathrm{o}}} = \frac{\varepsilon_i^{\mathrm{o}}(D_{ij} - \delta_{ij}) - \frac{\partial\varepsilon_i^{\mathrm{o}}}{\partial\beta_j^{\mathrm{o}}}(\varepsilon_i - \beta_i^{\mathrm{o}})}{(\varepsilon_i - \beta_i^{\mathrm{o}})^2}, \tag{38}$$

$$\frac{\mathrm{d}h_i}{\mathrm{d}\varepsilon_j^{\mathrm{o}}} = -\frac{2}{\sigma^u}\sigma_i^k E_i(D_{ij} - \delta_{ij}), \qquad \frac{\mathrm{d}h_i}{\mathrm{d}\beta_j^{\mathrm{o}}} = -\frac{2}{\sigma^u}\sigma_i^k E_i(D_{ij} - \delta_{ij}),$$

$$\frac{\mathrm{d}b_i}{\mathrm{d}\varepsilon_j^{\mathrm{o}}} = \frac{\partial\beta_i^{\mathrm{o}}}{\partial\varepsilon_j^{\mathrm{o}}}\sigma_i^{k'} + \beta_i^{\mathrm{o}}E_i(D_{ij} - \delta_{ij}), \qquad \frac{\mathrm{d}b_i}{\mathrm{d}\beta_j^{\mathrm{o}}} = \delta_{ij}\sigma_i^{k'} + \beta_i^{\mathrm{o}}E_i(D_{ij} - \delta_{ij}).$$

We can expect that in the final solution the following conditions have to be satisfied (for all load states) for elements $i \in B_2^k$ with active constraints (35)

$$\sigma_i^k = \sigma_i^{\mathrm{L}k} + \sum_j E_i(D_{ij} - \delta_{ij})(\varepsilon_j^{\mathrm{o}k} + \beta_j^{\mathrm{o}}) = \sigma^u \tag{39}$$

and the following conditions on active constraints (34) have to be satisfied for vanishing elements in all load states k:

$$\varepsilon_i^{\mathrm{o}k} = \varepsilon_i^k \quad \text{and} \quad \beta_i^{\mathrm{o}} = 0. \tag{40}$$

The sets B_2^k determine maximally loaded elements (dominant members) in each load state.

Note that some of the gradient formulas (38) contain the derivative $\partial\beta_i^{\mathrm{o}}/\partial\varepsilon_j^{\mathrm{o}}$ or $\partial\varepsilon_i^{\mathrm{o}}/\partial\beta_j^{\mathrm{o}}$. The distortion fields β_i^{o} and $\varepsilon_i^{\mathrm{o}}$ are conjugate through the yielding criterion (39). For the *modified structure*, where $\varepsilon_i^{\mathrm{o}}$ affects the stress formula in an implicit way (through modified deformations (cf. Eqs. $(25)_2$ for *distorted structure*), we get the following strains and stresses with respect to remodelled cross-sections A_i:

$$\begin{aligned} \sigma_i &= E_i(\varepsilon_i - \beta_i^{\mathrm{o}}) = E_i\left(\varepsilon_i^{\mathrm{L}} + \sum_j D_{ij}\varepsilon_j^{\mathrm{o}} + \sum_p (D_{ip} - \delta_{ip})\beta_p^{\mathrm{o}}\right), \\ \varepsilon_i &= \varepsilon_i^{\mathrm{L}} + \sum_j D_{ij}\varepsilon_j^{\mathrm{o}} + \sum_p D_{ip}\beta_p^{\mathrm{o}}. \end{aligned} \tag{41}$$

Substituting $(41)_1$ to (39) we obtain:

$$\sum_p B_{lp}\beta_p^{\mathrm{o}} + \sum_j D_{lj}\varepsilon_j^{\mathrm{o}} = -(\varepsilon_l^{\mathrm{L}} - \varepsilon^u), \quad \text{where} \quad B_{lp} = D_{lp} - \delta_{lp}. \tag{42}$$

Now, calculating derivatives with respect to $\varepsilon_j^{\mathrm{o}}$ (for any load state) we can get the following set of l' equations:

$$\sum_p B_{lp}\frac{\partial\beta_p^{\mathrm{o}}}{\partial\varepsilon_j^{\mathrm{o}}} = -D_{lj} \tag{43}$$

determining the missing derivatives $\partial\beta_p^{\mathrm{o}}/\partial\varepsilon_j^{\mathrm{o}}$ (where l' denotes number of damaged members and $l, p = 1, 2, \ldots, l'$).

6. Structural remodelling algorithms

The following five algorithms solving the optimal remodelling problem are proposed:

1. Gradient calculation + Sequential Quadratic Programming (GSQP)
2. Gradient calculation + Heuristic methods (GH)
3. Tracking active constraints + Heuristic methods (TH)

4. Elasto-Plastic multi-load case (EP)

5. Iterative Simplex (IS)

The GSQP approach is based on the assumption that goal function and constraint gradients of the problem (11), (12), (14) are calculated according to analytical formulas (see sections 4 and 5) and then optimization algorithm by K. Schittkowski (cf. Ref. [10]) is employed. This approach is incompetent in treating mechanical nuances of the remodelling task such as stress sign swap for instance. As far as "friendly" cases (pretty uniform stress distribution, no anticipated stress sign swap) are considered, the GSQP approach does its job very well for a single load state. The analysis of large structures may be time-taking though. For k load states the number of variables for n element structure increases k times and the number of constraints goes up by $3n(k-1)$, which results in considerable prolongation of computation time. There is also much to be wished about the quality of achieved results, since the optimization procedure sometimes fails to produce anticipated output. Being more specific it does not fulfill the requirement that each structure member must be strained to its limit in at least one of the applied load states.

In the GH approach (see Table 1) it is vital that advantage is taken of the mechanical features of the remodelling problem. Analytically calculated gradients are the basis for the original incremental

Table 1. Structural remodelling algorithm GH (single load case)

1) Calculate D matrix, calculate ε_i^L $\varepsilon_i = \varepsilon_i^L$, $\varepsilon_i^o = 0$, $B_1 = B_2 = O = \{0\}$, δ-small parameter
2) Search for $\Delta\varepsilon_i^o$ direction for $i \notin B_1 \cup B_2$ on the basis of Eq. (22) for $i \in B_1$ on the basis of Eqs. (22) and (23) or realizing $\varepsilon_i^o \Rightarrow \varepsilon_i$ for $i \in B_2$ on the basis of Eqs. (22) and (24) or realizing $\varepsilon \Rightarrow \varepsilon^u$ for $i \in O$, $\varepsilon_i^o = 0$
3) Determine the step $\Delta\varepsilon_i^o$
4) Calculate structural response $\varepsilon_i = \varepsilon_i + \sum_j D_{ij}\Delta\varepsilon_j^o$
5) If constraints (12), (14) are violated more than δ then reduce the step $\Delta\varepsilon_i^o$ length and go back to 4)
6) Verification of sets B_1, B_2, O if $i \notin B_1$ and constraint (12) is active (with accuracy δ) then $i \in B_1$ if $i \notin B_2$ and constraint (14) is active then $i \in B_2$ if $i \in B_1$ and constraint (12) is not active then $i \notin B_1$ if $i \in B_2$ and constraint (14) is not active then $i \notin B_2$ if $i \in O$ and $\lvert\varepsilon_i\rvert > \delta$ then $i \notin O$
7) Accumulation of distortions $\varepsilon_i^o = \varepsilon_i^o + \Delta\varepsilon_i^o$
8) Qualitative analysis VDM-Q if matrix $[D - I]$ defined for B_2 is singular and $\lvert\Delta\varepsilon_i^o\rvert < \delta$ then STOP else go back to 2)

algorithm in which the heuristic strategy of a vanishing member set is applied. If the ratio denoting the modification of cross sectional area drops beneath an arbitrarily chosen limit then the structure member is eliminated. For elements included in the set, the condition of zero element forces is imposed which significantly helps the algorithm convergence. This approach tackles the problem of stress sign swap very well thanks to "freezing" distortions whenever an element is suspected of this kind of behaviour. The algorithm is used to solve a single load case because it contains no heuristic knowledge about the imposed constraints. Since the character of the solution for a single load state is well known (isostatic substructure) the GH algorithm finds it by itself as the only possible one. However when analyzing large structures some problems may emerge due to diverse stress distribution. In this case a solution very close to the optimum can be returned.

The TH approach (see Table 2) relies on the heuristic algorithm for multi load cases. Unlike a single load case there is a necessity of tracking down active constraints when several load states are considered. Otherwise no convergence is achieved. First the dominant strain of k load states is determined for n structure members. Then the strategy of a vanishing member set, much the same as for the GH approach, is applied. After determining vanishing members the algorithm examines

Table 2. Structural remodelling algorithm TH (multi-load case)

1) Calculate D matrix, calculate ε_i^{Lk}, dominant states $\varepsilon_i^{Lk'}$ $\varepsilon_i^k = \varepsilon_i^{Lk}$, $\varepsilon_i^{k'} = \varepsilon_i^{Lk'}$, $\varepsilon_i^{ok} = 0$, $B_1 = B_2 = O = \{0\}$, δ-small parameter
2) Search for $\Delta\varepsilon_i^{ok'}$ direction (for each i according to the dominant states) for $i \notin B_1 \cup B_2$ on the basis of Eq. (22) for $i \in B_1$ on the basis of Eqs. (22) and (23) or realizing $\varepsilon_i^o \Rightarrow \varepsilon_i$ for $i \in B_2$ on the basis of Eqs. (22) and (24) or realizing $\varepsilon \Rightarrow \varepsilon^u$ for $i \in O$ $\varepsilon_i^o = 0$
3) Determine the steps $\Delta\varepsilon_i^{ok'}$ for dominant states then determine the remaining steps $\Delta\varepsilon_i^{ok'}$ from Eq. (18)
4) Calculate structural response $\varepsilon_i^k = \varepsilon_i^k + \sum_j D_{ij}\Delta\varepsilon_j^{ok}$
5) If constraints (12), (14) are violated more than δ then reduce the step $\Delta\varepsilon_i^{ok}$ length and go back to 4)
6) Verification of sets B_1, B_2, O if $i \notin B_1$ and constraint (12) is active for some load state then $i \in B_1$ if $i \notin B_2$ and constraint (14) is active for some load state then $i \in B_2$ if $i \in B_1$ and constraint (12) is not active for all load states then $i \notin B_1$ if $i \in B_2$ and constraint (14) is not active for all load states then $i \notin B_2$ if $i \in O$ and $\lvert\varepsilon_i\rvert > \delta$ for all load states then $i \notin O$
7) Accumulation of distortions $\varepsilon_i^{ok} = \varepsilon_i^{ok} + \Delta\varepsilon_i^{ok}$
8) Convergence check if $\lvert\Delta\varepsilon_i^o\rvert < \delta$ then STOP else go back to 2)

how far each remaining member is from the strain limit. Appropriate distortion increments are applied in order to reach the strain limit. This way the concept of tracking active constraints is realized. Missing $n(k-1)$ distortion increments for non-dominant states of load are calculated making use of the formula $\varepsilon_i^o = (1-\mu_i)\varepsilon_i$ as cross-sectional coefficients remain the same for all load states. This algorithm finds the solution in which every structure member is strained to its limit in at least one of the applied load states. One should be very careful however when setting the threshold for picking up vanishing members. If set improperly some constraints may appear not to be fulfilled at the end. An extra bonus of this algorithm is that the solution for a single load state can be obtained by inputting the same load state twice. This approach fails if applied load states cause very diverse stress fields in the structure. For large structures the problem of convergence may be troublesome.

The EP algorithm is the extension of the TH approach on elasto-plastic, multi-load case. In the EP algorithm (see Table 3) the simulation starts from optimally remodelled structure for

Table 3. Remodelling simulation algorithm EP (elasto-plastic, multi-load case)

1) Calculate D matrix, calculate ε_i^{Lk}, σ^{uu}-initial stress limit

$\varepsilon_i^k = \varepsilon_i^{Lk}$, $\varepsilon_i^{ok} = \beta_i^o = 0$, $B_2^k = \{0\}$, δ-small parameter

2) Multi-load remodelling with constant β_i^o and $\sigma^u = \sigma^{uu}$

determine sets of dominant members B_2^k for all load states

track active constraints $\Delta\varepsilon_i^{ok} = \varepsilon^u - \varepsilon_i^k$ for $i \in B_2^k$

Push down the stress limit σ^u

3) Determine the step $\Delta\sigma^u$

4) Update current stress limit $\sigma^u = \sigma^u - \Delta\sigma^u$

5) For all load states k simultaneously

calculate $\Delta\beta_i^{ok}$ for all elements from B_2^k basing on Eq. (39)

6) Accumulate plastic distortion increments $\Delta\beta_i^o = \sum_k \Delta\beta_i^{ok}$

7) If $|\Delta\beta_i^o| \geq \delta$ then go to 8)

if $\sigma^{uu} - \sigma^u < \delta$ then STOP else go back to 2)

8) Accumulation for all load states simultaneously

$\beta_i^o = \beta_i^o + \Delta\beta_i^o$

$\sigma_i^k = \sigma_i^k + \sum_j E_i(D_{ij} - \delta_{ij})\Delta\beta_j^o$

9) If constraints (35) are violated more than δ for any load state then

correct $\Delta\sigma_u$ and go back to 4)

elastic, multi-load case (fully stressed design). Having the solution, it is assumed that the arbitrarily imposed stress limit σ^u matches the yield limit. As a consequence fully stressed members in each of

the applied load states become plastified. Then we proceed to enlarge the plastic zone in each load state to its maximum. It can be done by gradual decreasing of the yield limit and repeating the TH simulation at each decrease. Finally we get a structure in which the plastic zone in every load state is spread over as many elements as possible. This is the optimal elasto-plastic, multi-load case structure. One must remember to do some rescaling of stresses and distortions at the end, which is due to lowering of the initial yield limit (see section 7.5).

In the IS approach (see Table 4) the classical simplex method is employed iteratively to the linearized problem (11)–(13), (15) subject to design variables ε_i^o and μ_i. Nonlinear constraints (15) can be written in the form:

$$\varepsilon_i^o = (1 - \mu_i)\varepsilon_i \,, \tag{44}$$

where ε_i is expressed by $(1)_2$. The constraints are linearized by keeping strains at iteration constant. The input variables for the simplex method are the cross-sectional redistribution coefficients μ_i and the current strains ε_i. The solution obtained after an iteration is processed in order to update states of strains and distortions. The algorithm is stopped when variable increments are sufficiently small. The main advantage of the approach is its being automatic. On the other hand it does not regard the remodelling problem as a mechanical one. Consequently the lack of quality analysis can be observed. It sometimes ends up with really bizarre solutions (loss of geometrical determinacy for instance). The IS algorithm can be adapted to the multi-load as well as elasto-plastic case.

Table 4. Remodelling simulation algorithm IS (single load, elastic case)

1) Calculate D matrix, calculate ε_i^L, ε^u-strain limit, δ-small parameter $\varepsilon_i = \varepsilon_i^L$, $\varepsilon_i^{ok} = 0$
2) Calculate distortions then update current strains $\varepsilon_j^o = (1 - \mu_j)\varepsilon_j$ $\varepsilon_i = \varepsilon_i^L + \sum_j D_{ij}(1 - \mu_j)\varepsilon_j$
3) Use SIMPLEX method to find $min \sum_i \mu_i A_i l_i$ subject to: $\mu_i \geq 0$ $\lvert\varepsilon_i^L + \sum_j D_{ij}(1 - \mu_j)\varepsilon_j\rvert \leq \varepsilon^u$ Solution provides μ_i
4) Check convergence if $\Delta\mu_i < \delta$ then STOP else go back to 2)

7. NUMERICAL EXAMPLES

7.1. Simple box truss structure

Let us consider the simple structure shown in Fig. 3 which is subjected to a single load state. Assuming the initial cross-sectional areas to be $A_1 = \ldots = A_3 = 0.02011$ cm^2 and $A_4 = A_5 =$

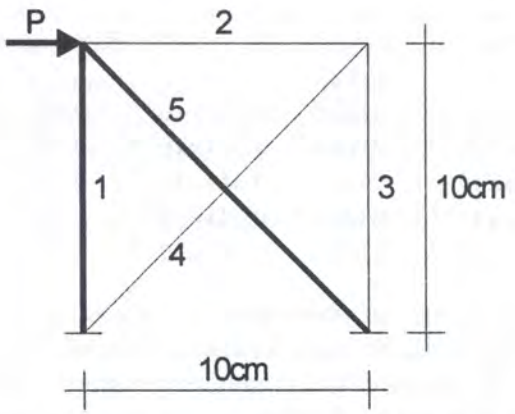

Fig. 3. Simple box truss structure under single load

0.02890 cm^2, the Young's modulus constant for all members $E = 10M$ Pa and the stress limit $\sigma^u = 3438.5$ Pa, the following stress and strain distribution within the elastic range is obtained:

	Initial structure		Distortions	Remodelled structure		Section change
Elem.	ε	σ [Pa]	ε	ε^0	σ [Pa]	μ
1	0.285×10^{-3}	2845.4	-0.154×10^{-3}	0.344×10^{-3}	4973.6	1.45
2	-0.213×10^{-3}	-2128.2	-0.232×10^{-3}	-0.232×10^{-3}	0.0	0.00
3	-0.213×10^{-3}	-2128.2	-0.232×10^{-3}	-0.232×10^{-3}	0.0	0.00
4	0.209×10^{-3}	2093.7	0.284×10^{-3}	0.284×10^{-3}	0.0	0.00
5	-0.280×10^{-3}	-2799.3	0.145×10^{-3}	-0.344×10^{-3}	-4893.0	1.42

The remodelling process leads to the isostatic substructure marked bold in Fig. 3. The total volume gets down from $V_{\text{initial}} = 1.42$ cm^3 to $V_{\text{final}} = 0.87$ cm^3. None of the final strain values exceeds the strain limit $\varepsilon^u = 0.34385 \times 10^{-3}$ according to problem corollaries. If the initial cross sections were changed as indicated above, all remaining members would reach the stress limit. This result could be obtained thanks to any of previously described numerical techniques since the structure consists of only five members.

Let us now analyze what happens to the structure after applying another symmetrical force as shown in Fig. 4.

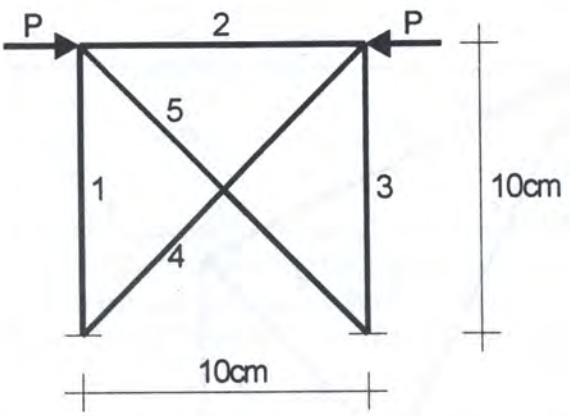

Fig. 4. Simple box truss structure under two load states

The initial state for the left force remains unchanged and for the right one becomes analogous due to the load symmetry. The results are filed for each load state respectively:

	Left force			Right force			Section change
Elem.	ε	ε^0	σ [Pa]	ε	ε^0	σ [Pa]	μ
1	0.344×10^{-3}	0.129×10^{-5}	3425.6	-0.255×10^{-3}	-0.096×10^{-5}	-2542.7	1.00
2	-0.344×10^{-3}	-0.132×10^{-3}	-2118.9	-0.344×10^{-3}	-0.132×10^{-3}	-2118.9	0.62
3	-0.255×10^{-3}	-0.096×10^{-5}	-2542.7	0.344×10^{-3}	0.129×10^{-5}	3425.6	1.00
4	0.255×10^{-3}	0.025×10^{-3}	2302.5	-0.344×10^{-3}	-0.034×10^{-3}	-3102.0	0.90
5	-0.344×10^{-3}	-0.034×10^{-3}	-3102.0	0.255×10^{-3}	0.025×10^{-3}	2302.5	0.90

In this case each of the structure members reaches its strain limit in at least one of the load states (member No. 2 in both states). No drop-outs are observed (Fig. 4). The material gain is very tiny (less than 1%) because all of the initial members remained. The remodelling process caused the best possible distribution of material. Even at such a simple example the GSQP method would encounter difficulties in reaching the exact solution. The above result was obtained with the help of the TH approach.

7.2. Ten-element truss structure

Let us now take into consideration the truss structure shown in Fig. 5 exposed to one vertical force. Assuming the initial cross-sectional areas to be $A_1 = \ldots = A_3 = 0.02011$ cm^2 and $A_4 = \ldots = A_10 = 0.02890$ cm^2, the Young's modulus constant for all members $E = 10$ MPa and the stress limit $\sigma^u = 3438.5$ Pa, the following stress and strain elastic distribution is obtained:

	Initial structure		Distortions	Remodelled structure		Section change
Elem.	ε	σ [Pa]	ε	ε^0	σ [Pa]	μ
1	-0.268×10^{-3}	-2678.5	-0.283×10^{-3}	-0.283×10^{-3}	0.0	0.00
2	0.038×10^{-3}	383.4	-0.147×10^{-3}	-0.147×10^{-3}	0.0	0.00
3	0.230×10^{-3}	2295.1	-0.154×10^{-3}	0.344×10^{-3}	4973.6	1.45
4	-0.163×10^{-3}	-1631.0	-0.018×10^{-3}	-0.344×10^{-3}	-3262.0	0.95
5	0.163×10^{-3}	1631.0	0.301×10^{-3}	0.301×10^{-3}	0.0	0.00
6	-0.436×10^{-3}	-4363.9	0.172×10^{-3}	-0.344×10^{-3}	-5157.7	1.50
7	0.099×10^{-3}	991.2	0.086×10^{-3}	0.344×10^{-3}	2578.8	0.75
8	-0.159×10^{-3}	-1587.6	-0.279×10^{-3}	-0.279×10^{-3}	0.0	0.00
9	0.079×10^{-3}	793.8	0.194×10^{-3}	0.194×10^{-3}	0.0	0.00
10	0.107×10^{-3}	1065.0	-0.235×10^{-3}	-0.235×10^{-3}	0.0	0.00

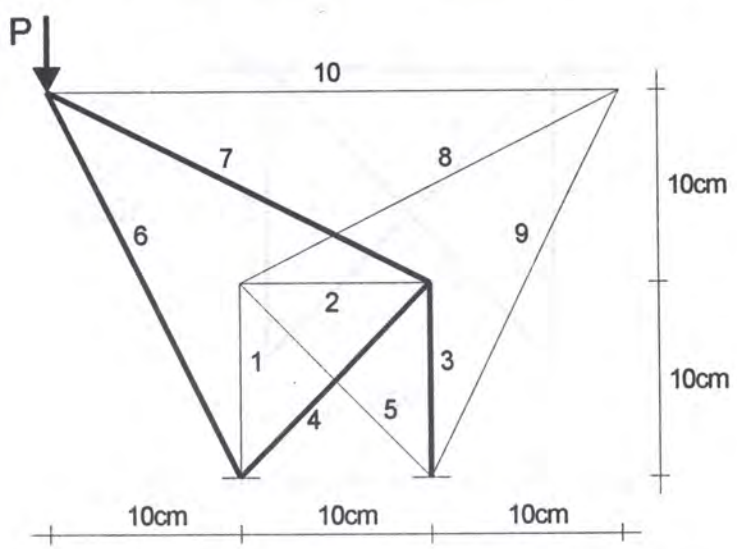

Fig. 5. 10-element truss structure under single load

During the remodelling process six out of ten elements are eliminated. The remaining ones create the isostatic substructure marked bold in Fig. 5 in which every member reaches the strain limit. The algorithm starts with the volume $V_{\text{initial}} = 4.87$ cm^3 and returns the volume $V_{\text{final}} = 2.13$ cm^3 which is a very considerable material gain. This result was achieved using the GH approach. The GSQP and the IS approaches are comparable in terms of computation time because the structure is still not complex.

Let us take a look now how the structure behaves under two symmetrical forces shown in Fig. 6.

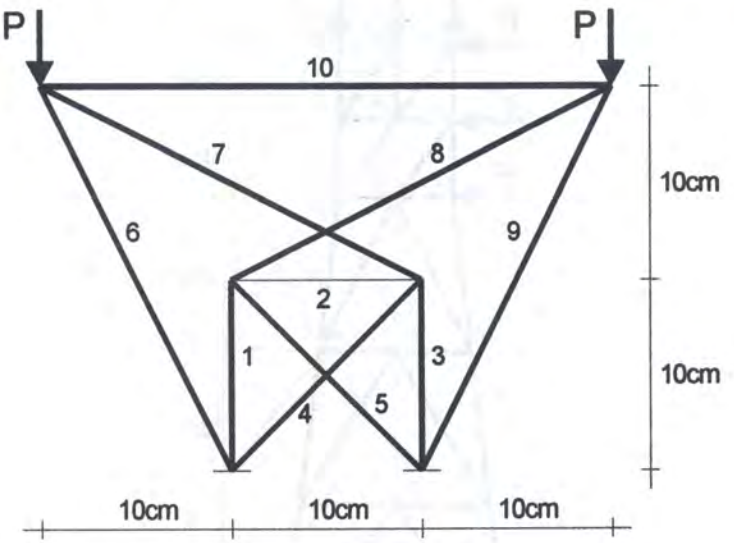

Fig. 6. 10-element truss under two load states

The remodelling analysis results for each load state are the following:

	Left force			Right force			Section change
Elem.	ε	ε^0	σ [Pa]	ε	ε^0	σ [Pa]	μ
1	-0.278×10^{-3}	-0.055×10^{-3}	-2221.4	0.344×10^{-3}	0.069×10^{-3}	2752.2	0.80
2	-0.199×10^{-3}	-0.199×10^{-3}	0.0	-0.199×10^{-3}	-0.199×10^{-3}	0.0	0.00
3	0.344×10^{-3}	0.069×10^{-3}	2752.2	-0.278×10^{-3}	-0.055×10^{-3}	-2221.4	0.80
4	-0.344×10^{-3}	-0.163×10^{-3}	-1805.1	0.278×10^{-3}	0.132×10^{-3}	1457.0	0.52
5	0.278×10^{-3}	0.132×10^{-3}	1457.0	-0.344×10^{-3}	-0.163×10^{-3}	-1805.1	0.52
6	-0.344×10^{-3}	0.114×10^{-3}	-4581.8	0.043×10^{-3}	-0.014×10^{-3}	575.9	1.33
7	0.344×10^{-3}	0.201×10^{-3}	1427.0	-0.278×10^{-3}	-0.162×10^{-3}	-1151.8	0.42
8	-0.278×10^{-3}	-0.162×10^{-3}	-1151.8	0.344×10^{-3}	0.201×10^{-3}	1427.0	0.42
9	0.043×10^{-3}	-0.014×10^{-3}	575.9	-0.344×10^{-3}	0.114×10^{-3}	-4581.8	1.33
10	0.344×10^{-3}	0.267×10^{-3}	772.7	0.344×10^{-3}	0.267×10^{-3}	772.7	0.22

Member No. 2 turned out to be unnecessary in the structure and was consequently eliminated. All other elements reach the strain limit in one of the load states (member No. 10 in both). The starting volume is $V_{\text{initial}} = 4.87$ cm^3 and the final volume is $V_{\text{final}} = 3.20$ cm^3. This means that getting rid of just one member, 34% of the initial material is spared. The result was achieved through the TH approach.

7.3. Offshore jacket

The next example shown in Fig. 7 has more to do with real projects. It is supposed to simulate the behaviour of an offshore jacket. The following data were taken into account: uniform Young's

modulus $E = 10$ MPa, the same cross-sectional area $A = 232$ cm^2, the stress limit $\sigma^u = 3500$ Pa. Each element is identified by the numbers of its nodes. The results of the single load case remodelling (Fig. 7) are shown in Appendix A.

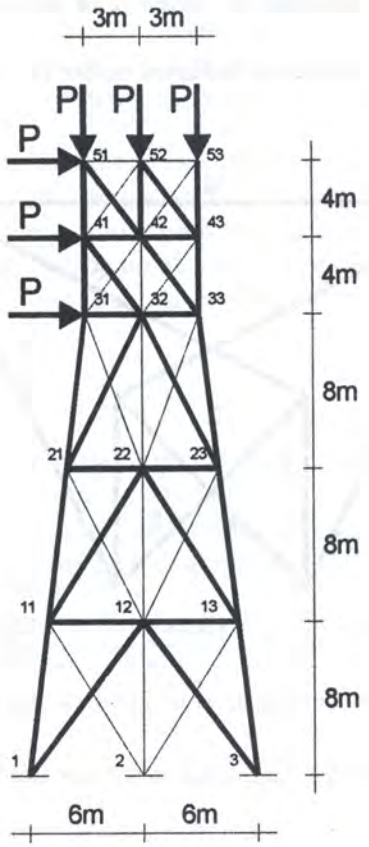

Fig. 7. Offshore jacket under one load state

The simulation started with the structure consisting of 45 elements contributing to the volume $V_{\text{initial}} = 6.56$ m^3 and ended up with the 29-element isostatic structure, marked bold in Fig. 7, of the final volume $V_{\text{final}} = 4.29$ m^3. This way 35% of the initial material is spared. The result can be achieved through the GSQP technique which takes approximately 3 minutes on PC Pentium 90. However the use of the GH approach in this case is recommended since it requires just one minute to return the result. Thus the superiority of heuristic methods is clear for large structures. Let us now consider how the behaviour of the offshore jacket changes after applying a symmetrical load state shown in Fig. 8.

This time the algorithm classifies only five members as being absolutely unnecessary. The remaining structure is marked bold in Fig. 8. However the solution is not perfect, because there are two members No. 3242 and 4252, marked with dotted lines in Fig. 8 and with asterisks in the results listing, which are maximally strained in neither of the load states. So according to the remodelling theory they should drop out (their final cross sections indicate so too). The results were achieved thanks to the GSQP approach and the above described inaccuracy is due to the Schittkowski's procedure which doesn't respect the mechanical context of the problem. Nevertheless the obtained solution is quite satisfactory since basing on it the character of the global optimum for the structure is likely to be predicted. The total volume gets down from $V_{\text{initial}} = 6.56$ m^3 to $V_{\text{final}} = 5.57$ m^3 that is to say 15% of the initial volume can be spared. The computations for the problem took about 15 minutes on PC Pentium 90 which is significantly longer than the time spent for calculating the same structure under one load state. The full list of results is shown in Appendix B.

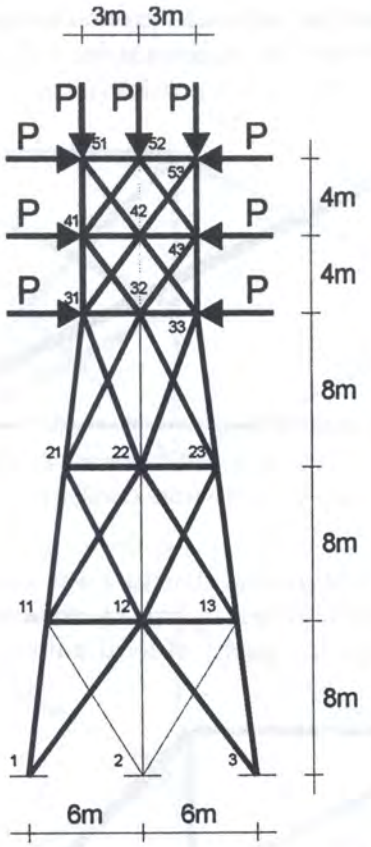

Fig. 8. Offshore jacket under two load states

7.4. Large truss cantilever

The intention of the example is to compare the VDM-obtained results with some literature ones (cf. Ref. [9]). A large truss cantilever subjected to one load state with different grid layouts is considered. The ground structure of the aspect ratio 8 : 5 for the 3×3 grid is shown in Fig. 9. The following input data were assumed: length $l = 24$ m, height $h = 15$ m, uniform Young's modulus

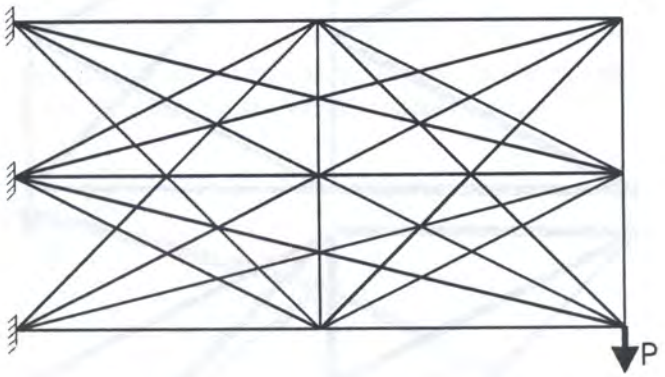

Fig. 9. Ground structure of the truss cantilever for the grid 3×3

$E = 1$ MPa, uniform initial cross-sectional areas $A = 2.545$ cm^2, yield limit $\sigma^u = 100$ Pa, applied load $P = 0.1$ N.

Let us make a comment on the ground structure definition, introduced by Dorn (cf. Ref. [11]). In this paper all overlapping as well as support-support members are excluded from consideration.

Thus by applying the 2×2 grid the 5-element ground structure was reduced to the 2-element optimal truss, shown in Fig. 10, whose final volume is $V_2 = 91.80 \times 10^3$ cm^3.

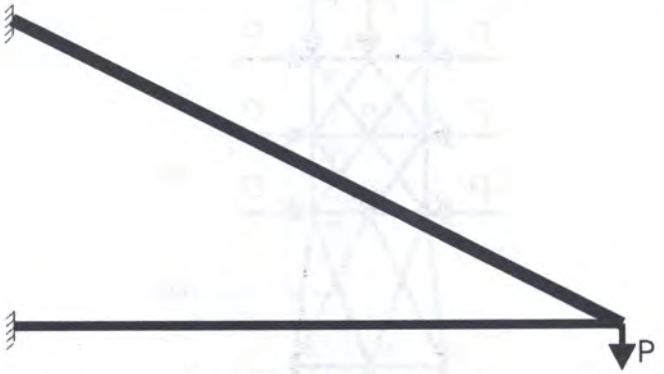

Fig. 10. Optimal topology of the truss cantilever for the grid 2×2 (GH)

Then the 3×3 grid with 26-element ground structure was analyzed (see Fig. 9). Three equivalent (in terms of total volume) topologies, shown in Fig. 11, were found ($V_3 = 87.60 \times 10^3$ cm^3). This indicates that the objective function has plenty of local minima, very close to one another.

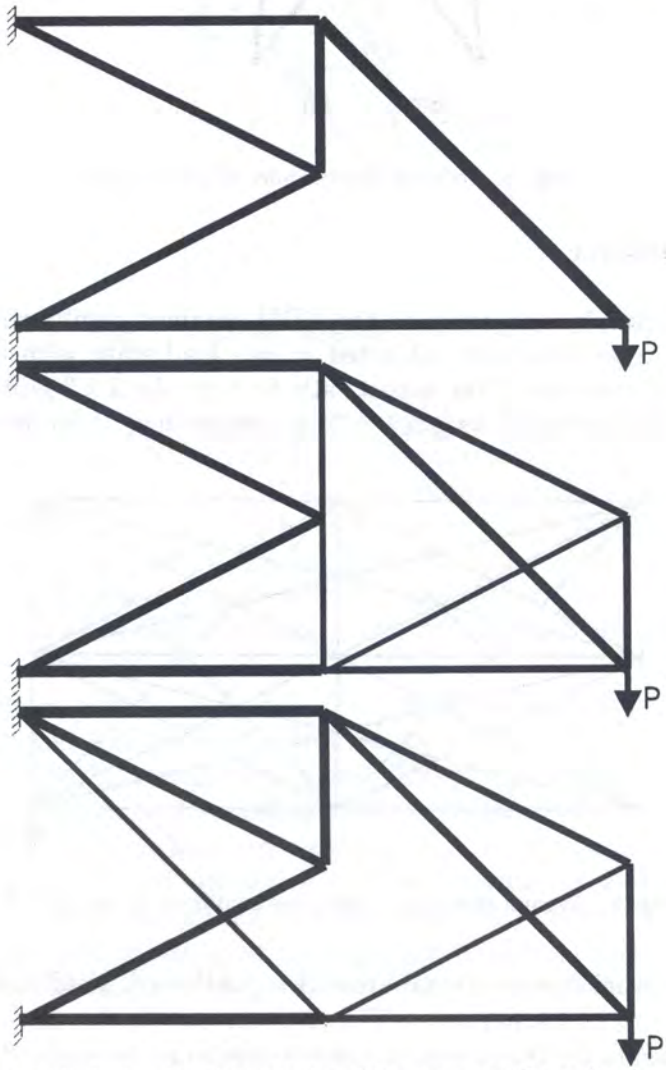

Fig. 11. Three equivalent optimal topologies of the truss cantilever for the grid 3×3 (GH)

As a comparison the literature solution (cf. Ref. [9]), shown in Fig. 12, was taken. Since the redundancy of the literature topology equals two, the truss was further optimized by the GH algorithm, resulting in the statically determinate structure, shown in Fig. 13.

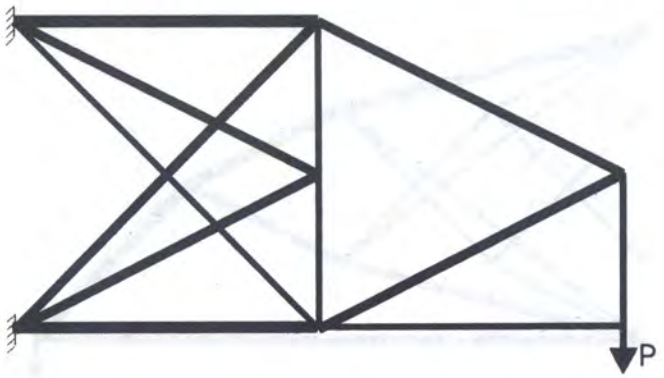

Fig. 12. Optimal literature topology of the truss cantilever for the grid 3 × 3

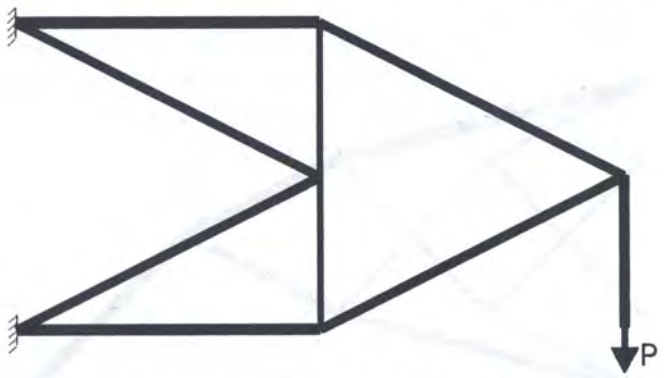

Fig. 13. VDM-improved literature topology of the truss cantilever for the grid 3 × 3

The truss shown in Fig. 13 is geometrically indeterminate. However the fact can be ignored in this case taking into account the load direction. The final volume of the structure reached the value $V_{3m} = 87.60 \times 10^3$ cm^3, which is exactly the same we got previously by starting with the 26-element ground structure (compare V_3).

At the last stage of analysis the 5 × 5 grid was chosen. Due to considerable computation time the limited number of 136 connections in the ground structure was considered (instead of 196). The GH algorithm, employed for solution, produced the optimal truss of the volume $V_5 = 80.61 \times 10^3$ cm^3, shown in Fig. 14.

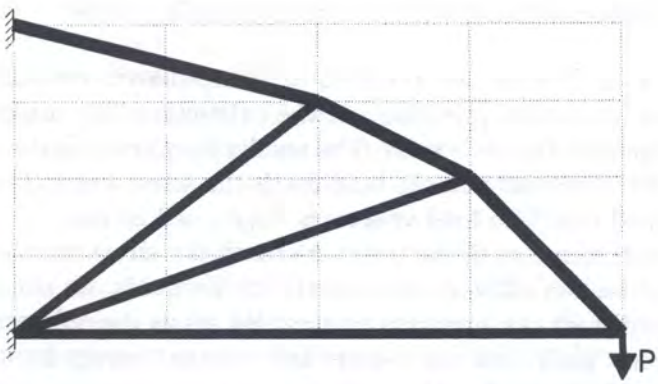

Fig. 14. Optimal topology of the truss cantilever for the grid 5 × 5 (GH)

As a comparison the literature solution (cf. Ref. [9]), shown in Fig. 15, was examined. The redundancy of the structure is two, so the truss was optimized by the GH algorithm in order to make it statically determinate. The result is presented in Fig. 16.

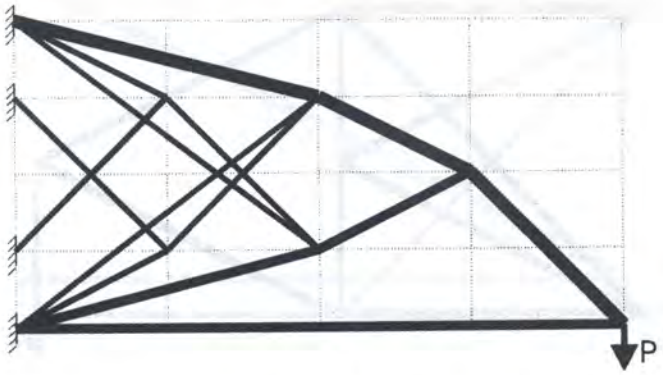

Fig. 15. Optimal literature topology of the truss cantilever for the grid 5 × 5

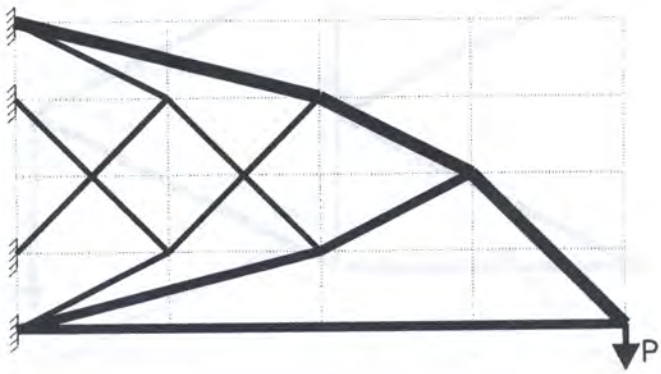

Fig. 16. VDM-improved literature topology of the truss cantilever for the grid 5 × 5

The final volume of the VDM-improved literature topology for the 5×5 grid is $V_{5m} = 80.26 \times 10^3$ cm^3. Thus we see that the volume V_5, achieved by the GH algorithm from the 136-element ground structure, exceeds V_{5m} by only 0.4%.

The structure in Fig. 14 is more attractive than the one in Fig. 16 from the point of view of real application whereas their volumes are almost the same.

7.5. Ten-element truss structure within elasto-plastic range

Let us have a closer look now at the problem of elasto-plastic remodelling, analyzing the 10-element truss structure (described previously in the subsection 7.2) subjected to two symmetrical load states. All data assumed before is valid. The results for purely elastic part of the redesign task are presented in Fig. 17. Elements marked bold reach the stress limit. The element No. 2, marked by a dotted line, dropped out. The final volume is $V_{\text{elastic}} = 3.20$ cm^3.

In order to make more elements of the structure reach the stress limit we can now proceed three different paths. Firstly, we can allow natural plasticity. Secondly, we can apply structural fuses in selected members. Thirdly, we can prestress element No. 10 as the only remaining symmetrical one in the structure. The first path does not require any external energy input. However it is not easy to handle numerically. The second path needs an optimization procedure in order to locate the fuses. As for the third path, the analysis boils down to just one member. It is also quite likely to

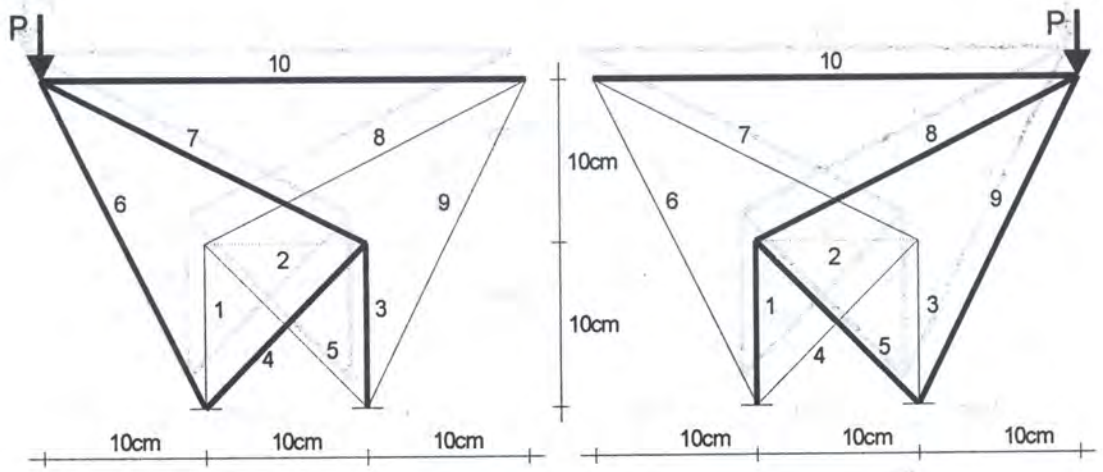

Fig. 17. 10-element truss structure after elastic remodelling

be applied in real-life projects. Eventually all of these paths lead to the same final volume. Thus our attention will be focused on the second and the third one. In numerical algorithm we introduce prestress by generating a distortion in No. 10, opposite in sign to the elastic stress in that member. This is performed by gradual increase of the stress limit, which causes equivalent effect. These are the final results:

	Left force			Right force			Plastic-like	Section
No.	σ_e [Pa]	ε^0	σ_{ep} [Pa]	σ_e [Pa]	ε^0	σ_{ep} [Pa]	β^0	μ
1	-2775.4	-0.697×10^{-4}	-3803.1	3438.5	0.697×10^{-4}	3804.0	0.0	0.82
2	0.0	-0.003×10^{-4}	0.0	0.0	-0.003×10^{-4}	0.0	0.0	0.00
3	3438.5	0.697×10^{-4}	3804.0	-2775.4	-0.697×10^{-4}	-3803.1	0.0	0.82
4	-3438.5	-0.697×10^{-4}	-3804.0	2775.4	0.697×10^{-4}	3803.1	0.0	0.82
5	2775.4	0.697×10^{-4}	3803.1	-3438.5	-0.697×10^{-4}	-3804.0	0.0	0.82
6	-3438.5	-0.417×10^{-4}	-3804.0	432.2	0.060×10^{-4}	543.4	0.0	0.89
7	3438.5	0.697×10^{-4}	3804.4	-2775.4	-0.697×10^{-4}	-3803.1	0.0	0.82
8	-2775.4	-0.697×10^{-4}	-3803.1	3438.5	0.697×10^{-4}	3804.0	0.0	0.82
9	432.2	0.060×10^{-4}	543.4	-3438.5	-0.417×10^{-4}	-3804.0	0.0	0.89
10	3438.5	-0.045×10^{-4}	3804.0	3438.5	-0.045×10^{-4}	3804.0	-0.199×10^{-3}	1.01

As a result 8 members of the structure reach (due to prestress) the stress limit (Fig. 18), increased by 10.6% in comparison with the initial one. Since we have reached a higher stress limit we now need to bounce back to the initial one, by multiplying cross-sections indicated in the above table by $\sigma_{ep}/\sigma_e = 1.106$ and the prestress distortion in element No. 10 by $\sigma_e/\sigma_{ep} = 0.904$. Then the total volume gets down to $V_{\text{elasto-plastic}} = 3.08$ cm^3, which gives 4% material gain.

The same final volume can be obtained by introducing two structural fuses in elements No. 4 and 5 which have the biggest potential contribution to energy dissipation of all members in the structure (in other words, plastic distortions generated in members 4 and 5, needed to bring the largest portion of the structure to yielding, are the smallest). In numerical algorithm the initial stress limit is gradually decreased (eventually down by 13,4%), which finally results in bringing 8 elements to yielding at a lower stress level. After rescaling the final cross-sections (multiplying by coefficient $\sigma_{ep}/\sigma_e = 0.866$) and plastic distortions (multiplying by coefficient $\sigma_e/\sigma_{ep} = 1.155$) we arrive at the structure with 8 elements reaching the initial stress limit. The final volume is $V_{\text{elasto-plastic}} = 3.08$ cm^3 as in previous example. The results of the simulation are as follows:

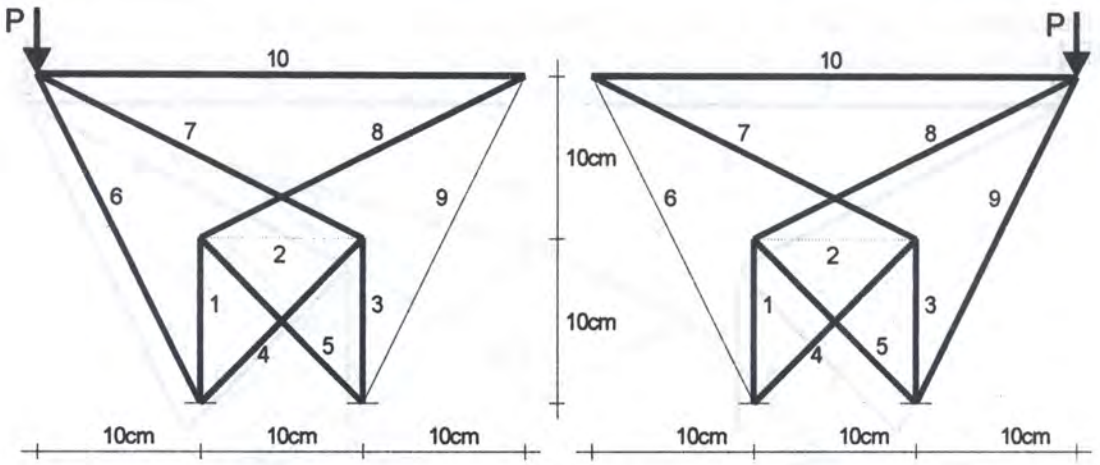

Fig. 18. 10-element truss structure after elasto-plastic remodelling

	Left force			Right force			Plastic-like	Section
No.	σ_e [Pa]	ε^0	σ_{ep} [Pa]	σ_e [Pa]	ε^0	σ_{ep} [Pa]	β^0	μ
1	-2775.4	0.131×10^{-4}	-2976.2	3438.5	-0.131×10^{-4}	2976.4	0.0	1.04
2	0.0	-0.351×10^{-3}	0.0	0.0	-0.351×10^{-4}	0.0	0.0	0.00
3	3438.5	-0.131×10^{-4}	2976.4	-2775.4	0.131×10^{-4}	-2976.2	0.0	1.04
4	-3438.5	0.131×10^{-4}	-2976.4	2775.4	-0.131×10^{-4}	2976.2	-0.175×10^{-3}	1.04
5	2775.4	-0.131×10^{-4}	2976.2	-3438.5	0.131×10^{-4}	-2976.4	-0.175×10^{-3}	1.04
6	-3438.5	0.411×10^{-4}	-2976.4	432.2	-0.059×10^{-4}	425.2	0.0	1.14
7	3438.5	-0.131×10^{-4}	2976.4	-2775.4	0.131×10^{-4}	-2976.2	0.0	1.04
8	-2775.4	0.131×10^{-4}	-2976.2	3438.5	-0.131×10^{-4}	2976.4	0.0	1.04
9	432.2	-0.059×10^{-4}	425.2	-3438.5	0.411×10^{-4}	-2976.4	0.0	1.14
10	3438.5	-0.873×10^{-4}	2976.4	3438.5	-0.873×10^{-4}	2976.4	0.0	1.29

8. Conclusions

Numerical efficiency of the VDM approach to simulation of optimal structural remodelling through virtual distortions is due to the following properties:

- analytical formulation with direct mechanical interpretation of particular steps in the remodelling simulation process
- analytical sensitivity analysis
- versatility of the VDM approach enabling combined simulation of the remodelling process for multi-load as well as elasto-plastic cases.

Saving of total material volume due to the optimal remodelling applied to elasto-plastic structures is relatively low. However, the main potential application of such formulated design strategy can be significant expansion of the plastic zone under extreme loading. As a consequence, it means higher dissipation of the impact energy and improved structural safety. Installing so called *structural fuse devices* (cf. Ref. [8]) built into the structural elements and allowing for controlled plastic-like yielding, an adaptive structure with higher load capacity can be designed.

Acknowledgements

This paper presents a part of the results of the COPERNICUS 150 Project "Design of Offshore Structures under Extreme Wave Loading" (started in February 1995), supported by the financial contribution from the commission of the European Communities DGXII and from the partners in the project: UBI (Portugal), IFTR (Poland), TUP (Poland), CU (UK), BSHC and SRDI (Bulgaria). This paper presents a part of the Ph.D. thesis of the first author, supervised by the second author.

APPENDIX A

	Initial structure		Remodelled structure		Section change
Elem.	ε	σ [Pa]	ε	σ [Pa]	μ
111	0.808×10^{-3}	8082.6	0.350×10^{-3}	7829.4	2.24
112	0.310×10^{-3}	3100.0	0.350×10^{-3}	2158.0	0.62
211	0.099×10^{-3}	990.2	-0.256×10^{-3}	0.0	0.00
212	-0.108×10^{-3}	-1078.0	0.0	0.0	0.00
213	-0.209×10^{-3}	-2088.9	0.256×10^{-3}	0.0	0.00
312	-0.448×10^{-3}	-4479.9	-0.350×10^{-3}	-2158.0	0.62
313	-1.016×10^{-3}	-10164.4	-0.350×10^{-3}	-13049.0	3.73
1112	-0.194×10^{-3}	-1941.3	-0.350×10^{-3}	-1294.8	0.37
1121	0.629×10^{-3}	6285.3	0.350×10^{-3}	5219.6	1.49
1122	0.309×10^{-3}	3093.3	0.350×10^{-3}	3053.8	0.87
1213	0.319×10^{-3}	3192.6	0.350×10^{-3}	1294.8	0.37
1221	0.395×10^{-5}	39.5	-0.280×10^{-3}	0.0	0.00
1222	-0.108×10^{-3}	-1080.7	0.0	0.0	0.00
1223	-0.127×10^{-3}	-1270.8	0.280×10^{-3}	0.0	0.00
1322	-0.440×10^{-3}	-4396.4	-0.350×10^{-3}	-3053.8	0.87
1323	-0.819×10^{-3}	-8192.3	-0.350×10^{-3}	-10439.2	2.98
2122	-0.110×10^{-3}	-1104.6	-0.350×10^{-3}	-1294.8	0.37
2131	0.341×10^{-3}	3411.8	0.350×10^{-3}	1739.9	0.50
2132	0.323×10^{-3}	3227.4	0.350×10^{-3}	3860.4	1.10
2223	0.224×10^{-3}	2243.6	0.350×10^{-3}	1942.2	0.55
2231	-0.162×10^{-3}	-1617.6	-0.187×10^{-3}	0.0	0.00
2232	-0.081×10^{-3}	-813.4	0.0	0.0	0.00
2233	0.015×10^{-3}	152.0	0.187×10^{-3}	0.0	0.00
2332	-0.457×10^{-3}	-4571.1	-0.350×10^{-3}	-5790.6	1.65
2333	-0.522×10^{-3}	-5217.5	-0.350×10^{-3}	-5219.6	1.49
3132	-0.136×10^{-3}	-1362.3	-0.350×10^{-3}	-1510.6	0.43
3141	0.103×10^{-3}	1034.8	0.350×10^{-3}	1726.4	0.49
3142	0.105×10^{-3}	1045.0	0.294×10^{-3}	0.0	0.00
3233	0.081×10^{-3}	807.3	0.350×10^{-3}	1510.6	0.43
3241	-0.176×10^{-3}	-1759.3	-0.350×10^{-3}	-2158.0	0.62
3242	-0.096×10^{-3}	-957.7	-0.044×10^{-3}	0.0	0.00
3243	0.044×10^{-3}	437.4	0.350×10^{-3}	0.0	0.00
3342	-0.251×10^{-3}	-2513.1	-0.350×10^{-3}	-3596.7	1.03
3343	-0.302×10^{-3}	-3024.4	-0.350×10^{-3}	-2301.9	0.66
4142	-0.076×10^{-3}	-758.9	-0.350×10^{-3}	-431.6	0.12
4151	-0.049×10^{-3}	-490.0	-0.044×10^{-3}	0.0	0.00
4152	0.015×10^{-3}	146.8	-0.154×10^{-3}	0.0	0.00
4243	0.051×10^{-3}	506.2	0.350×10^{-3}	431.6	0.12
4251	-0.155×10^{-3}	-1545.5	-0.350×10^{-3}	-2158.0	0.62
4252	-0.082×10^{-3}	-819.0	-0.350×10^{-3}	-1151.0	0.33
4253	-0.959×10^{-5}	-95.9	0.022×10^{-3}	0.0	0.00
4352	-0.128×10^{-3}	-1281.1	-0.350×10^{-3}	-719.3	0.21
4353	-0.165×10^{-3}	-1649.7	-0.350×10^{-3}	-1726.4	0.49
5152	-0.080×10^{-3}	-799.1	-0.350×10^{-3}	-431.6	0.12
5253	0.576×10^{-5}	57.6	-0.016×10^{-3}	0.0	0.00

APPENDIX B

Elem.	Initial structure ε	Initial structure σ [Pa]	Remodelled structure ε	Remodelled structure σ [Pa]	Section change μ
111	0.216×10^{-3}	7965.7	-0.350×10^{-3}	-12912.7	3.69
112	0.299×10^{-3}	1988.9	-0.350×10^{-3}	-2327.1	0.66
211	-0.307×10^{-3}	0.0	-0.227×10^{-3}	0.0	0.00
212	-0.040×10^{-3}	0.0	-0.040×10^{-3}	0.0	0.00
213	-0.227×10^{-3}	0.0	-0.307×10^{-3}	0.0	0.00
312	-0.350×10^{-3}	-2327.1	0.299×10^{-3}	1988.9	0.66
313	-0.350×10^{-3}	-12912.7	0.216×10^{-3}	7965.7	3.69
1112	-0.298×10^{-3}	-913.4	0.350×10^{-3}	1074.6	0.31
1121	0.199×10^{-3}	6124.7	-0.350×10^{-3}	-10746.6	3.07
1122	0.298×10^{-3}	2154.2	-0.350×10^{-3}	-2534.6	0.72
1213	0.350×10^{-3}	1074.6	-0.298×10^{-3}	-913.4	0.31
1221	-0.350×10^{-3}	-823.8	0.222×10^{-3}	521.4	0.24
1222	-0.073×10^{-3}	0.0	-0.073×10^{-3}	0.0	0.00
1223	0.222×10^{-3}	521.4	-0.350×10^{-3}	-823.8	0.24
1322	-0.350×10^{-3}	-2534.6	0.298×10^{-3}	2154.2	0.72
1323	-0.350×10^{-3}	-10746.6	0.199×10^{-3}	6124.7	3.07
2122	-0.193×10^{-3}	-822.7	0.350×10^{-3}	1491.0	0.43
2131	0.123×10^{-3}	1933.5	-0.350×10^{-3}	-5486.3	1.57
2132	0.252×10^{-3}	3825.9	-0.350×10^{-3}	-5314.4	1.52
2223	0.350×10^{-3}	1491.0	-0.193×10^{-3}	-822.7	0.43
2231	-0.350×10^{-3}	-416.1	0.060×10^{-3}	71.7	0.12
2232	-0.108×10^{-3}	0.0	-0.108×10^{-3}	0.0	0.00
2233	0.060×10^{-3}	71.7	-0.350×10^{-3}	-416.1	0.12
2332	-0.350×10^{-3}	-5314.4	0.252×10^{-3}	3825.9	1.52
2333	-0.350×10^{-3}	-5486.3	0.123×10^{-3}	1933.5	1.57
3132	-0.350×10^{-3}	-1504.6	0.154×10^{-3}	660.2	0.43
3141	0.129×10^{-3}	1310.1	-0.350×10^{-3}	-3555.7	1.02
3142	0.042×10^{-3}	273.5	-0.350×10^{-3}	-2276.4	0.65
3233	0.154×10^{-3}	660.2	-0.350×10^{-3}	-1504.6	0.43
3241	-0.350×10^{-3}	-2323.8	0.133×10^{-3}	881.0	0.66
3242	-0.273×10^{-3}	-177.1	-0.273×10^{-3}	-177.1	0.06*
3243	0.133×10^{-3}	881.0	-0.350×10^{-3}	-2323.8	0.66
3342	-0.350×10^{-3}	-2276.4	0.042×10^{-3}	273.5	0.65
3343	-0.350×10^{-3}	-3555.7	0.129×10^{-3}	1310.1	1.02
4142	-0.250×10^{-3}	-141.0	0.350×10^{-3}	197.6	0.06
4151	-0.055×10^{-3}	-294.1	-0.350×10^{-3}	-1882.6	0.54
4152	0.092×10^{-3}	-318.6	-0.350×10^{-3}	-1210.4	0.35
4243	0.350×10^{-3}	197.6	-0.250×10^{-3}	-141.0	0.06
4251	-0.350×10^{-3}	-1790.4	0.038×10^{-3}	195.2	0.51
4252	-0.299×10^{-3}	-503.3	-0.299×10^{-3}	-503.3	0.17*
4253	0.038×10^{-3}	195.2	-0.350×10^{-3}	-1790.4	0.51
4352	-0.350×10^{-3}	-1210.4	0.092×10^{-3}	-318.6	0.35
4353	-0.350×10^{-3}	-1882.6	-0.055×10^{-3}	-294.1	0.54
5152	-0.350×10^{-3}	-652.2	0.063×10^{-3}	-117.1	0.19
5253	0.063×10^{-3}	-117.1	-0.350×10^{-3}	-652.2	0.19

REFERENCES

[1] A.G.M. Michell. The Limits of Economy of Material in Frame Structures. *Phil. Mag.*, **8**: 589–597, 1904.

[2] M.P. Bendsoe, A. Ben-Tal, J. Zowe. Optimization Methods for Truss Geometry and Topology Design. *Structural Optimization*, **7**: 141–159, 1994.

[3] M.P. Bendsoe, N. Kikuchi. Generating Optimal Topologies in Structural Design Using a Homogenization Method. *Computer Methods in Applied Mechanics and Engineering*, **71**: 197–224, 1988.

[4] T. Lewiński, M. Zhou, G.I.N. Rozvany. Extended Exact Solutions for Least-Weight Truss Layouts. *International Journal of Mechanical Sciences*, **36**: 375–398, 1994

[5] B.M.V. Topping. Mathematical Programming Techniques for Shape Optimization of Skeletal Structures. In: G.I.N. Rozvany, ed., *Shape and Layout Optimization in Structural Design*, 349–376. Springer, Vienna, 1992.

[6] J. Holnicki-Szulc, J.T. Gierliński. *Structural Analysis, Design and Control by the Virtual Distortion Method.* J. Wiley & Sons, Chichester, 1995.

[7] J. Holnicki-Szulc. Optimal Structural Remodelling — Simulation by Virtual Distortions. *Communications in Applied Numerical Methods*, Vol. 5, 289–298, 1989.

[8] J. Holnicki-Szulc, F. Lopez Almansa. Optimal Design of Adaptive Structures. *Proc. 1st World Congress of Structural and Multidisciplinary Optimization*, Goslar, May 1995.

[9] S. Sankaranarayanan, R.T. Haftka, R.K. Kapania. Truss Topology Optimization with Simultaneous Analysis and Design. *AIAA Journal*, **32**(2): 420–424, 1994.

[10] K. Schittkowski. *NLPQL: A Fortran Subroutine Solving Constrained Nonlinear Programming Problems.* Report of Institute of Informatics, Univ. of Stuttgart, Germany, 1993.

[11] W.S. Dorn, R.E. Gomory, H.J. Greenberg. Automatic Design of Optimal Structures. *Journal de Mecanique*, **3**(1): 25–52, 1964.